ULTRA-SHALLOW JUNCTION FORMATION BY POINT DEFECT ENGINEERING and ULTRA LOW ENERGY BORON IMPLANTS

L. Shao[1], J. Chen[2], J.M. Zhang[2], D. Tang[2], W.K. Chu[1]
[1]*Department of Physics, and Texas Center for Superconductivity and Advanced Materials, University of Houston, Houston, Texas 77204*
[2]*Advanced Ion Beam Technology, Inc., San Jose, CA 94086*

Abstract – Fabrication of ultra-shallow junctions with low contact resistances is desired to advance current CMOS technology beyond the 90 nm technology node. The traditional method of low energy B implantation followed by rapid thermal annealing is unsatisfactory for the following two reasons: (i) a low level of electrical activation, limited by the solid solubility of B in Si and (ii) too deep a junction depth due to undesirable dopant diffusion resulting from interactions with Si interstitials. Furthermore, beam current is inevitably low in sub-keV B implantation due to space charge limitation, making this a time-consuming processing step. Currently, deceleration of boron, after mass selection, is used to provide adequate beam current. However, the energy contamination introduced can significantly degrade the junction formations. In the first part of the present study, we investigated the effects of energy monochromaticity of B ion beams on junction formation. It shows that energy contamination at 0.05% ??? and above can broaden the post-annealing B profile appreciably into deeper regions. In the second part, we demonstrated ultra-shallow junction formation by combining the techniques of point defect engineering (PDE) and ultra low energy (< 500 eV) B implantation. This approach is based on the earlier finding that high-energy ion bombardment with silicon can create spatially separated distributions of interstitials and vacancies, with a vacancy rich region near the surface. Boron diffusion is retarded in this vacancy rich surface region so that the dopant profile remains localized at the surface. Moreover, boron activation is enhanced beyond that expected from its solid solubility. Using PDE together with highly monoenergetic ultra-low energy B implantation we have fabricated the most shallow boron junction with a dopant distribution profile closest to the ideal box-like form.

I. Introduction

To meet the demanding scaling requirements for complimentary metal oxide semiconductor (CMOS) devices beyond the 90 nm node [1], significant technological barriers have to be overcome. The traditional method of low energy B implantation followed by rapid thermal annealing encounters three serious difficulties. One is a low level of electrical activation limited by the solid solubility of boron in silicon. Another is the anomalous boron diffusion due to interactions with Si interstitials [2-4]. Last, but not least is the low beam current available in ultralow energy implantation due to space charge effects. One method of achieving adequate boron beam current is the use of deceleration technology. Starting with a beam extracted from the source at a higher energy, a reverse bias is applied to decelerate the ions down to the final desired energy. The final beam current achievable by deceleration is higher than that obtained by

extracting the ions at the desired final energy but charge exchanges and neutral transport during deceleration can give rise to energy contaminated beams. The dopant tail profile itself is not significant if the contamination level is low. However, the much higher damage level coming from high energy contamination in the incident ion beam increases the transient enhanced diffusion of B more than proportionately, resulting in considerable boron diffusion. Therefore, control of energy contamination is very critical to device fabrication, since damage induced by energy contamination can degrade device performance further, e.g. by increasing leakage current, if the damage is not annealed out completely.

In the present study, we studied the sensitivity of boron diffusion to beam energy purity. This will provide an idea of how important the accuracy of implantation control should be. Then we proceed to the study the use of point defect engineering (PDE) to control boron diffusion.

II. Experimental Results on Effects of Energy Contamination on Junction Formation

Bare (100)-oriented *n*-type Si wafers, preamorphized with 5 keV Ge ions of a dosage of $1\times10^{15}/cm^2$, were implanted with 0.2 keV B and 0.5 keV B, respectively, at a dosage of $5\times10^{14}/cm^2$. B implantation was performed using a high beam current, ultra low energy implanter (Advanced Ion Beam Technology, Inc., San Jose, CA). A 4 keV B^{11} beam is extracted from the accelerator and retarded by a potential of 3.5 keV for 0.5 keV B implantation. Intentional beam contamination was introduced by turning off the retarding potential to allow the 4 keV boron ions to irradiate the Si wafer directly. The percentage of contamination is defined as the ratio of the 4 keV B dose to that of the 0.5 keV B dose. Energy contamination, at levels of 0.05, 0.2, 0.3, and 0.4% was introduced. Rapid thermal annealing (RTA) of all the implanted samples were performed under N_2 ambient at 1050ºC for 1s. The B atomic depth distribution profiles were obtained using quadrupole secondary ion mass spectrometry (SIMS). ^{10}B and ^{11}B were monitored as positive ions under oxygen bombardment at an impact energy of 500 eV in the normal direction. Secondary ions were collected from the center 10% of a 450 μm × 450 μm rastered area. Oxygen flooding was used to reduce secondary ion transient effects near the surface. The depth scale was established using stylus profilometry on sputtered craters and assuming a constant sputtering rate. The atomic concentration of ^{10}B and ^{11}B were calculated from relative sensitivity factors determined from a standard sample.

Figure 1 shows the B profile of samples implanted with 0.5 keV B of a dosage of $5\times10^{14}/cm^2$. Profiles corresponding to energy contamination levels of 0.2, 0.3, and 0.4% were superimposed for comparison. As-implanted profiles of the energy contaminated samples have visible enhanced tails with buried peaks at around 17 nm deep, which corresponds to the implanted 4 keV B. Effects of various percentages of energy contamination on boron diffusion after RTA at 1050ºC in N_2 are surprisingly large. This is manifest in the data on display in Fig. 1. Energy contamination extends the junction depth significantly deeper than that obtained with monoenergetic implants. For the 0.2% contaminated sample, the junction depth measured at $1\times10^{18}/cm^3$, is increased by around 10 nm. The junction becomes much deeper as the percentage of contamination is further increased. Junction depth finally reaches 53 nm at 0.4% energy contamination,

corresponding to a diffusion length of almost double that obtained in samples with no energy contamination. The effects of energy contamination on 0.2 keV B implantation are shown in Figure 2. Even with energy contamination at 0.2%, B profiles extends significantly deeper. These results clearly show the importance of beam energy monochromaticity on the ultra shallow junction formation of devices beyond 90nm.

It is expected that B transient enhanced diffusion (TED) is absent in sub-keV implantation due to the proximity of the surface [5]. However, anomalous diffusion of B persists [6]. Several mechanisms are proposed. One is the so called boride-enhanced diffusion (BED) in which self interstitials injected from a silicon boride phase cause enhanced B diffusion [6]. Another is the coupled diffusion of B [7]. A simplifed explanation of the later mechanism is that the flux of B-self interstitial pairs into the bulk drags Si interstitials along, creating a concentration of Si self-interstitials above the equilibrium concentration of Si interstitials in the bulk. The Si surface concentration is assumed to be fixed at its equilibrium value. Thus the Si surface is a source of interstitials [7]. However, both of the above mechanisms are only operative at high B concentration, but not in the low B concentrations typical of the tail of the B profiles. We believe that the observed boron diffusion induced by energy contamination of the incident beam is mainly due to transient enhanced diffusion caused by additional implantation damage from 4 keV B bombardment.

Our studies have shown that energy contamination during decelerated ion implantation can affect adversely the post-annealing diffusion of B implants. In order to satisfy device requirements, highly monochromatic beams are needed.

III. Ultra Shallow Junction Formation by Point Defect Engineering

PDE [8,9] has been applied in this study to form ultra-shallow junctions with sub-keV B implants. PDE can reduce boride-enhanced diffusion, sharpen the B profile and enhance boron activation.

We have shown the retardation of boron diffusion from surface deposited B (deposited by electron-gun evaporation) on Si using point defect engineering (PDE) [8,9]. PDE using high-energy (MeV) ion implantation provides a unique method to separate the spatial distribution of vacancies and interstitials [10,11]. During ion bombardment, the forward momentum imparted to the lattice Si causes the recoiled Si interstitial distribution to be deeper than that of vacancies. Since spatially separated Frenkel pairs recombine in nearby proximity, an excess vacancy rich region is formed close to the surface and excess interstitials are left in the deep range [10,11]. Figure 3 shows excess vacancies caused by 1 MeV, $1\times10^{16}/cm^2$ Si ion implantation, calculated using the TRIM code [12]. The excessive vacancies have a concentration peaked around $2\times10^{20}/cm^3$ near the surface, and the concentration is slowly decreased to around $2\times10^{19}/cm^3$ and remains positive (vacancy rich) to around 0.9 μm deep.

Reduction of boron TED with co-implantation of MeV Si ions has been reported previously [13-18]. It should be emphasized that previous work have concentrated only on the diffusion of TED with B energy at a few keV to 40 keV, instead of desired sub-keV B implants while BED dominates the contribution to junction spreading than TED.

In this study, bare (100)-oriented n-type Si wafers, preamorphized with 5 keV Ge ions, were implanted with 0.5 keV B at a dosage of 1×10^{15} or $5\times10^{14}/cm^2$. A subset of the wafers additionally received a "PDE" MeV Si ion implantation with a dosage of $5\times10^{15}/cm^2$. RTA is performed under N_2 ambient at 900°C for 10s, 1000°C for 1s, and 1050°C for 1s, respectively.

Figure 4, 5, and 6 shows SIMS profiles of 0.5 keV B implants after 900, 1000 and 1050°C RTA. It shows that: 1) PDE significantly reduces B diffusivity. After 1000°C RTA, junction depth X_j (measured at $1\times10^{18}/cm^3$) is reduced from 30.8 nm (without PDE) to 21.4 nm (with PDE). B diffusivity is reduced by a factor of 22; 2) PDE make B profile sharper, by changing profile slope from 13.2 nm/decade to 4.7 nm/decade after 1000°C RTA; 3) PDE enhances B solid solubility. Diffusion of B in PDE sample starts from a concentration much higher than that of control samples. Equilibrium B solid solubility C_s in Si is $6.3\times10^{19}/cm^3$ at 900°C and $1.2\times10^{20}/cm^3$ at 1000°C [19]. For control sample, B profiles show a static peak and a rapidly diffusing B tail. Diffusion of B was limited below a concentration C_{diff}, which is around $6.1\times10^{19}/cm^3$ for 900°C and $7.0\times10^{19}/cm^3$ for 1000°C. For PDE sample, the critical value C_{diff} was enhanced to be $1.6\times10^{20}/cm^3$ at 900°C and $1.8\times10^{20}/cm^3$ at 1000°C. The values are larger than the solubility C_s by a factor of 2.6 and 1.5, respectively. For higher temperature RTA at 1050°C, C_{diff} is below C_s. This is due to the depletion of diffusible boron near the surface. Electrical measurement shows that the sheet resistances are 888 (at 1000°C) and 970 (at 900°C) ohm/square for control samples, while the values are reduced to 658 (at 1000°C) and 676 ohm/square (at 900°C) respectively for PDE samples. To match sheet resistance values, we divided the SIMS profiles by multiple small boxes with the unknown carrier concentration near surface region as a fitting parameter. It shows that boron activation of PDE sample is around $1.4\times10^{20}/cm^3$ for 1000°C and $1.3\times10^{20}/cm^3$ for 900°C. Still, these two values are larger than the solubility limit reported in the literature.

In most cases, electrical measurement of implanted B after annealing showed boron was not fully activated. A static, electrically inactive B peak was usually observed above a critical concentration which is below solid solubility of B in Si. B clustering can be described as [20]

$$B_S + I \leftrightarrow B_I, \qquad (1)$$

$$B_S + mB_I \leftrightarrow B_C + nI, \qquad (2)$$

where B_S refers to substitutional B atoms, B_I to mobile B atoms and B_C to immobile clusters containing $(m+1)$ B atoms, while n is the number of interstitials ejected upon clustering. The B clusters are metastable and would dissolve upon further high temperature annealing. Our study shows that activation of boron beyond solid solubility is possible with PDE. Previous study, although showing the enhanced activation of B, was unable to observe this phenomenon since the relative low dosage of B used is unable

to satisfy $C_B > C_s$ after RTA. With vacancy concentration significantly above the thermodynamical equilibrium value, PDE can 1) cause under-saturation of self

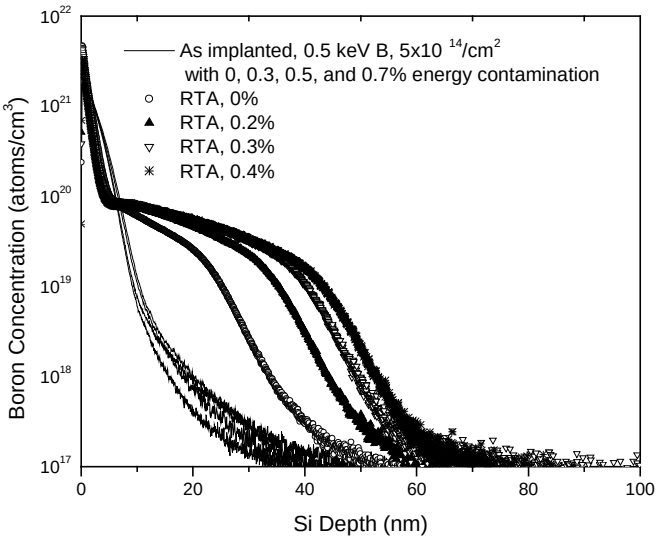

Figure 1. SIMS profiles of 0.5 keV B implants with a dosage of $5\times10^{14}/cm^2$, as implanted and annealed after 1050 ^oC RTA for 1s. Effects of various percent of energy contamination on boron diffusion are compared.

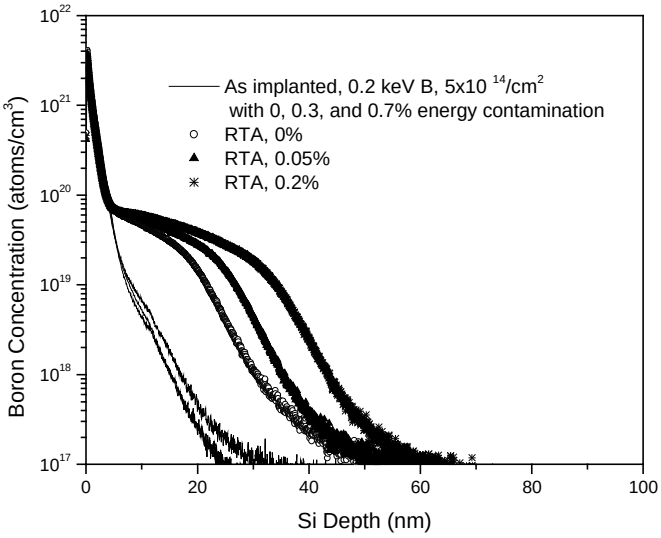

Figure 2. SIMS profiles of 0.2 keV B implants with a dosage of $5\times10^{14}/cm^2$. Effects of various percent of energy contamination on boron diffusion after 1050 ^oC for 1s are compared.

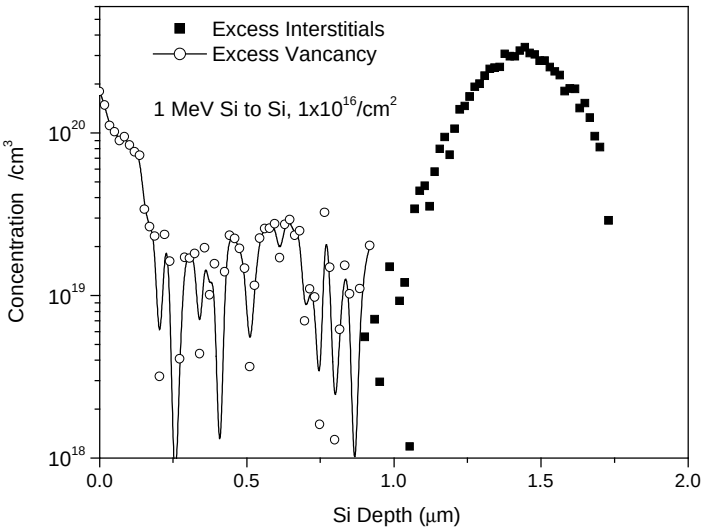

Fig. 3. TRIM simulation of defect imbalance after 1-MeV Si ion bombardment.

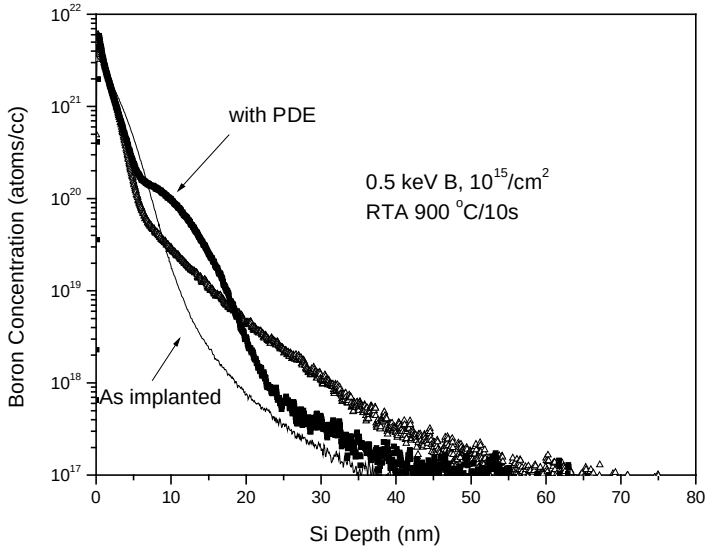

Fig. 4. SIMS profiles of $1\times10^{15}/cm^2$, 0.5 keV B implants, with or without MeV Si co-implantation, after annealing at 900 ^{o}C for 10s.

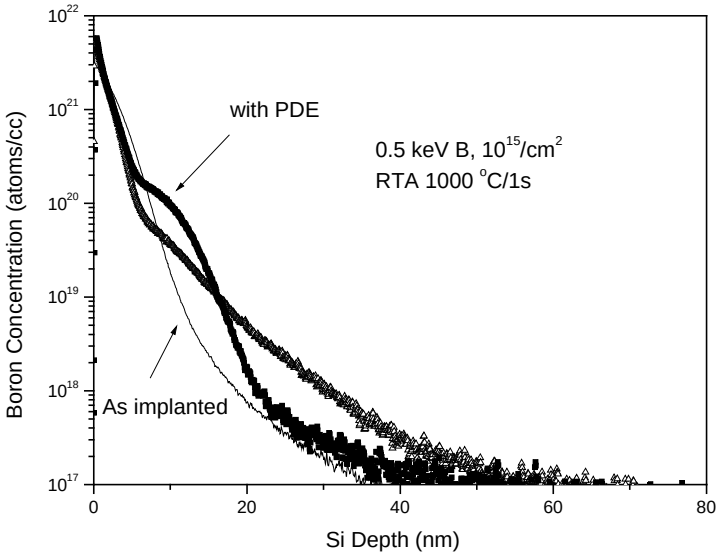

Fig. 5. SIMS profiles of $1\times10^{15}/cm^2$, 0.5 keV B implants, with or without MeV Si co-implantation, after annealing at 1000 ^{o}C for 1s.

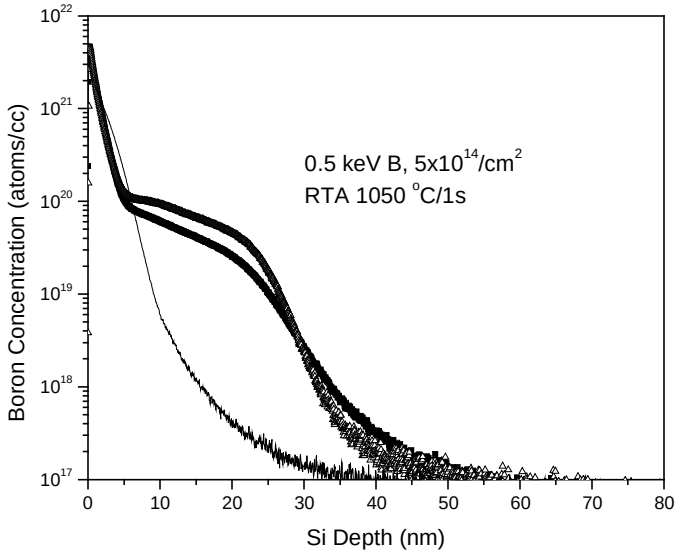

Fig. 6. SIMS profiles of $5\times10^{14}/cm^2$, 0.5 keV B implants, with or without MeV Si co-implantation, after annealing at 1050 ^{o}C for 1s.

interstitials, 2) promote dissolution of B in Si, 3) enhance B substitutional ratio and 3) reduce boron diffusion. The net result is the creation of an ultra shallow supersaturated B solution in Si using PDE.

IV. Conclusion

In summary, we have shown that energy contamination introduced by deceleration technology for increasing the beam currents available for low energy boron implants, can affect fabricated junctions adversely. Energy contamination at a level of 0.3% can extend the profile of 0.5 keV B implants 10 nm deeper after a 1050ºC spike annealing. A highly monoenergetic beam with energy contamination less than 0.1% is required for sub-micron devices. Furthermore, we have used PDE to control boron diffusion. PDE can reduce boron clustering and enhance boron activation. After annealing 0.5 keV B implanted samples over the wide temperature range of 750 to 1000°C, B activation has been enhanced. The enhancement factor is 2.6 at 900°C. Diffusion of B in the tail region has been reduced significantly and the boron profile is much sharper. The samples also exhibit a lower sheet resistance. We conclude that shallower and sharper box-like boron junctions can be achieved by PDE with sub-keV B implants with highly monoenergetic beams.

Acknowledgement

The study was supported in part by the State of Texas through the Texas Center for Superconductivity and Advanced Materials at the University of Houston. Portion of the work (Wei-Kan Chu) is also supported by his endowment from the Robert A. Welch Foundation.

References

1. The National Technology Roadmap for Semiconductor Industry Association, 2002, website: http://public.itrs.net
2. P.M. Fahey, P.B. Griffin, and J.D. Plummer, Rev. Mod. Phys. 61, 289 (1989).
3. N.E.B. Cowern, Phys. Rev. Lett 65, 2434 (1990).
4. P.A. Stolk, H-J, Gosssmann, D.J. Eaglesham, D.C. Jacobson, C.S. Rafferty, G.H. Gilmer, M.Jaraiz, J.M. Poate, H.S. Luftman, and T.E. Haynes, J. Appl. Phys. 81, 6031(1997).
5. Aditya Agarwal, H.-J. Gossmann, D. J. Eaglesham, S. B. Herner, A. T. Fiory, and T. E. Haynes, Appl. Phys. Lett. **74**, 2435 (1999).
6. Aditya Agarwal, H.-J. Gossmann, D.J. Eaglesham, S.B. Herner, A.T. Fiory, and T.E. Haynes, Appl. Phys. Lett 74, 2331(1999).
7. A. Ural, S. Koh, P.B. Griffin and J. D. Plummer, Mat. Res. Soc. Symp. V610, B4.11.1.
8. Lin Shao, X. Lu, J. Yue, Q. Li, J. Liu, P. A. W. Heide and W. K. Chu, Appl. Phys. Lett. 74, 3953(2000).

9. Lin Shao X. Lu, X. Wang, I. Rusokeva, J. Liu and W. K. Chu, Appl. Phys. Letter. 76, 2321(2001).
10. K.B. Winterbon, Radiat. Eff. 46, 181(1980).
11. M. D. Giles, J. Electrochem. Soc. 138, 1160 (1991).
12. J.P. Biersack and L.G. Haggmark, Nucl. Instrum. Methods 174, 257(1980)
13. V. Raineri, R.J. Schreutelkamp, F.W. Saris, K.T.F. Jansen, and R.E. Kaim, Appl. Phys. Lett. 58, 922(1991).
14. S.Saito, M.Kumagai and T.Kondo, Appl. Phys. Lett. 63, 197(1993).
15. K.K.Larsen, V.Privitera, S.Coffa, F.Priolo, C.Spinella, M.Saggio and S.U.Campisano, Nucl. Instrum. and Methods in Phys. Res. B. 112, 139(1996).
16. O.W. Holland and C.W. White, Nucl. Instrum. Methods Phys. Res. B 59/60, 353 (1991).
17. E.G. Roth, O.W. Holland, V.C. Venezia, and B. Nielsen, J. Electron. Mater. 26, 1349(1997).
18. V.C. Venezia, T.E. Haynes, A.Agarwal, L. Pelaz, H.-J. Gossmann, D.C. Jacobson, and D.J. Eaglesham, Appl. Phys. Lett. 74, 1299(1999).
19. R.B. Fair, J. Electrochem. Soc. 137, 667 (1990).
20. L. Pelaz, M. Jaraiz, G.H. Gilmer, H.-J. Gossmann, C.S. Rafferty, D.J. Eaglesham and J.M. Poate, Appl. Phy. Lett. 70, 2285(1997).